

# DERIVATION OF VELOCITY OF THE POTSDAM GLACIER, EAST ANTARCTICA USING SAR INTERFEROMETRY

Shridhar D. Jawak<sup>1</sup>, Prashant H. Pandit<sup>2</sup>, Alvarinho J. Luis<sup>1</sup>, Kapil Malik<sup>3</sup>, and V. S. P. Sinha<sup>2</sup>

<sup>1</sup>Polar Remote Sensing Section, Earth System Science Organization (ESSO), National Centre for Antarctic and Ocean Research (NCAOR), Ministry of Earth Sciences (MoES), Government of India, Headland Sada, Vasco-da-Gama, Goa-403804, India, Email: shridhar.jawak@gmail.com, alvluis1@gmail.com

<sup>2</sup>Department of Natural Resources, TERI University, New Delhi-110 070, India, Email: prashant.pandit@outlook.com, sinhav@teriuniversity.ac.in

<sup>3</sup>Radar System & Services, Muzaffarnagar, UP, India, Email: kapil@radarsystems.in

**KEYWORDS:** InSAR, interferometry, glacier velocity, Sentinel-1.

## ABSTRACT

The Synthetic Aperture Radar Interferometry (InSAR) is a robust method for monitoring Earth's surface mainly to measure its topography and deformation. It is a widely used technique in multidisciplinary applications. By using two SAR images interferogram was generated which showed phase as well as the amplitude information. The phase information from two and more interferogram further used to extract information about height and displacement of the surface. We used this technique to derived glacier velocity for Potsdam glacier which is located south of the Schirmacher oasis and north of Wohlthat Massif, east Antarctica, using Sentinel-1 Single Look Complex images captured in Interferometric Wide mode. For velocity estimation, Persistent Scatterer interferometry (PS-InSAR) method was applied. This method uses time coherent of permanent pixel of master images and correlates to same pixel of the slave image to get displacement. C-band sensor of European Space Agency, Sentinel-1A and 1B data were used in this study. Estimated average velocity was around 0.12 m/day, which varied annually from 30 to 60 m. The velocity varied by about 30-35 m/yr at higher elevation to 55-60 m/yr at lower elevation of the Potsdam glacier.

## 1. INTRODUCTION

Synthetic Aperture Radar interferometry (InSAR) is the very useful technique for measurement of topography and deformation of the earth surface. It is an active microwave radar imaging system, which works on Doppler motion principle. It uses two SAR images to generate interferogram. It uses InSAR capabilities in measuring and detection ground surface deformation up to sub-centimeter level on wide scale. Several studies have been carried out successfully for monitoring of the earth surface deformation caused by numerous sources like ice motion, subsidence phenomena, earthquake, volcano, etc. Radio Detection and Ranging (RADAR) is one of the primary tool for measuring distance of object from space, and the Synthetic Aperture Radar (SAR) is an advanced system that records phase as well as the amplitude information, where the phase is the number of cycles of oscillation of waves between radar and the surface. SAR data consist of a grid of complex values related to each pixel of a frame and it is possible to associate a phase value and an amplitude value connected to a reflected RADAR signal. Phase information enables to measure the distance between the radar antenna and a target, while amplitude values are influenced by the reflectivity of the target and give an indication of the power of the backscattered signal. InSAR estimates the phase difference between two SAR acquisitions, related to the variation of the sensor-target distance; if a temporal stack of SAR acquisitions is available, Differential InSAR (DInSAR) techniques could be applied to define the spatio-temporal evolution of an instability phenomenon, describing its deformation path. Cryospheric regions employ a wide variety of SAR and NISAR techniques (Jawak and Luis, 2014; Jawak et al., 2015a; Jawak et al., 2015b; Jawak and Luis, 2015c; Jawak and Luis, 2015d). The contribution of the SAR techniques for the cryosphere research includes measurement of the flow of glacier and ice sheet, generation of high resolution topographic maps, calculation of surface displacement associated with crustal deformation (Goldstein and Werner, 1998). Rapid movement of the flowing ice creates spectacular fringes pattern in interferogram, and it increase with increase in velocity. Monitoring of such high motion by satellite radar interferometry needs small orbital and temporal separation between consecutive passes (Massonnet and Feigl, 1998). Sequence of differential interferogram such as DInSAR or DiffSAR) is the effective technique of InSAR for the monitor the temporal behavior of the change detection that leads to generation of the time series which allows to monitor deformation (Berardino et al., 2002). The temporal gap of repeat-pass interferometry with marginal repetition of either days, months, or even years can be used for long-term observing of geodynamic phenomenon. DInSAR is able to measure displacements to centimeter accuracy, but depends upon the correlation (coherence) between RADAR acquisitions (higher coherence leads to better result). Persistent or Permanent Scatterer Interferometry (PS Interferometry) allows monitoring subsidence effect with millimeter accuracy. The processing system of PSI are

developed to cope with a single dominant point scattered inside a resolution cell, so as the number of interferogram increases the PS density improves. The recognition and the quantification of the glacier surface deformation using SAR interferometry technique having great impact in accuracy of results. Phase difference between two SAR images taken with some temporal gap with different view angle of the sensor has been used to measure the velocity of ice sheets and movement of glacier in polar region as well as Himalayan atmosphere. InSAR phase is sensitive to both coherent displacement and surface topography along the SAR look vector occurring between the acquisitions of the InSAR image pair (Kenyi and Kaufmann, 2003). Coherence tracking and intensity tracking, two cross correlation techniques applied to SAR dataset, to produce 2D vector field datasets have been combined with InSAR. If two or more radar images having good correlation and the orbital, topographic, tropospheric contributions can be modeled, the precision of InSAR is in the order of millimeter, sometimes other errors may arise while resolving the phase ambiguity through the unwrapping process (Berthier et al., 2005). The coherence over the glacier surface is affected by flow condition and meteorological parameter, and diminishes with increase in time interval between SAR images used to generate interferogram. Meteorological parameter, which create de-correlation, include surface melt of snow and ice and possibly snowfall and sometimes wind flow redistribution of snow and ice. De-correlation caused due to the glacier motion are incoherent displacements of adjacent scatterers and rapid flow if local deviations from the overall images registration function are not considered (Strozzi et al., 2002). Current work focuses on the estimation of glacier velocity in Antarctic region. The study is focused on (a) estimation of the velocity of Potsdam Glacier, (b) detecting the temporal velocity changes, and (3) quantifying the changes occurred within the region.

## 2. STUDY AREA

The Potsdam glacier is located south of the Schirmacher oasis and north of Wohlthat Massif. Most part of this glacier is above 1000 m above mean sea level; the annual air temperature is below  $-20^{\circ}\text{C}$  (Anschütz et al., 2007). The Indian Antarctic research station Maitri is located northwest,  $\sim 45$  km from this glacier. Geographically it extends from  $71.25^{\circ}\text{S}$  to  $71^{\circ}\text{S}$  and  $11^{\circ}\text{E}$  to  $12^{\circ}\text{E}$ , as it is shown in figure 2. The surface elevation varies from 1350 m above mean sea level in south-western part to nearly 600 m above sea level in the north-eastern part. The velocity of this glacier claimed 20-30 m/yr at higher region and 70-80 m/yr at lower region. The thickness of the ice is nearly  $>1200$  m. Accumulation dominates in south-western part of the glacier field, but there is some exception of small ablation zone near nunataks.

## 3. METHODOLOGY

This work is divided into a three-step process, (1) Data selection, (2) Data processing, (3) Product validation. For SAR data processing, it is important to have correct sets of data according to research requirement and the study area. Having adequate SAR images is the first sign of getting good results. In this study we used Sentinel-1 SAR interferometric single look complex data (SLC) level-1 product. For Potsdam glacier, six images were available which are listed in Table 1.

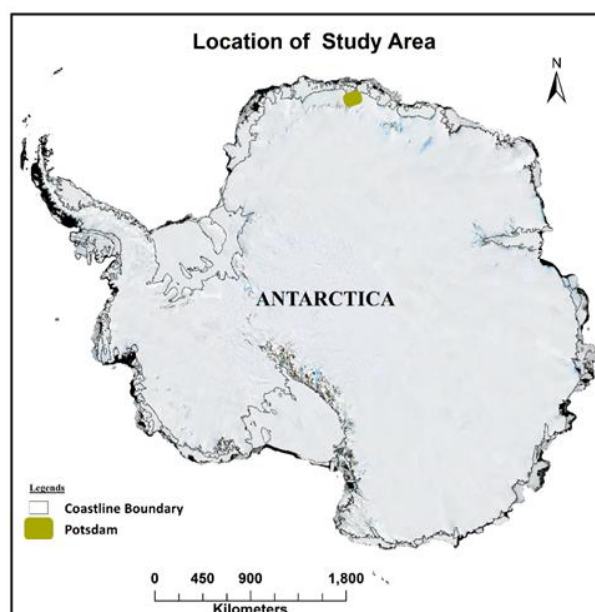


Figure 1. Location of Potsdam glacier, Antarctica

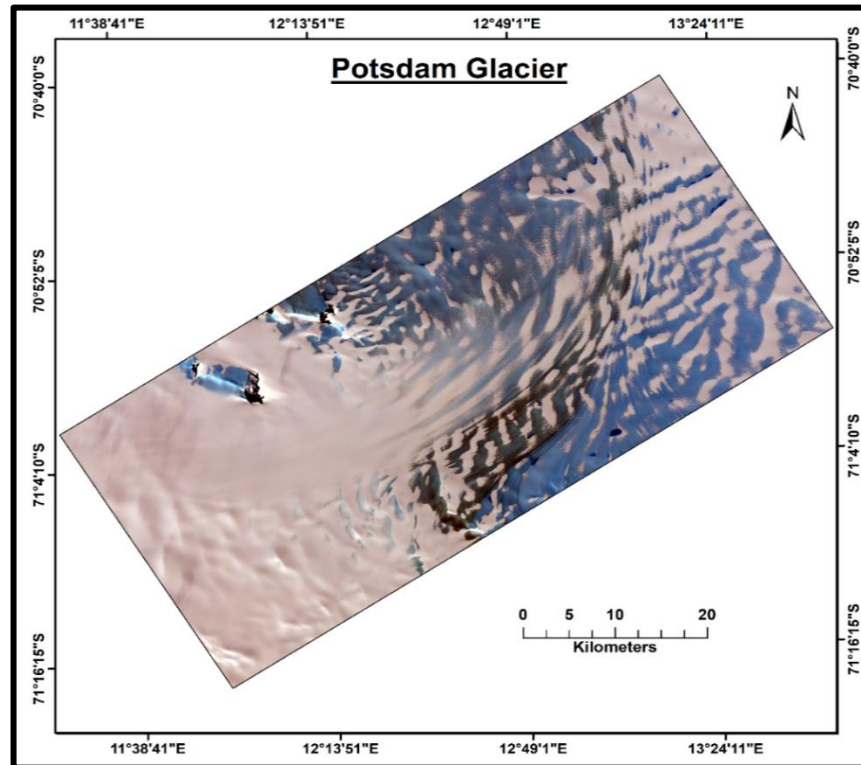


Figure 2. False colour combination map of Potsdam Glacier

Table 1. Details of Sentinel-1 SAR images used derive Potsdam glacier surface velocity.

Mission	Acquisition date	Orbit no	Id	Unique identifier	Flight Direction
S1A	29-07-2016	012367	01345C	7530	Ascending
S1A	10-08-2016	012542	013A32	2113	Ascending
S1A	22-08-2016	012717	014004	DC32	Ascending
S1A	03-09-2016	012892	0145EB	575B	Ascending
S1A	15-09-2016	013067	014B7D	DBCA	Ascending
S1A	27-09-2016	013242	015149	CE44	Ascending

### 3.1. Data processing

Interferometric Processing of SAR data for DEM generation as well as velocity calculation having some common steps like image co-registration, interferogram generation, interferogram flattening and topographical phase removal, phase unwrapping, height or velocity conversion and geo-coding.

### 3.2. Processing steps for velocity calculation

The derive velocity of glacier surface we used the persistent scatterer interferometric (PSInSAR or PSI) method where all SAR SLC images are taken for co-registration. For the PSI method, the number of images affects the accuracies of the results, because the co-registration depends upon the amplitude of the signal. The software used to generate velocity map from the SAR data has its own inbuilt module to handle every step of the functions and the function is further parted in sub-function as shown in Figure 3.

Input SLC images for PS processing begin with TOPS co-registration based on the geometry using orbit and External DEM; by exploiting the burst overlap and by using only stable area, the estimation of the azimuth co-registration residuals error occurs due to geometry. In second step, selection of Master and Slave is performed according to the need and availability. Before performing third step there is need of sparse point selection based on amplitude stability and reflective maps. These all sub-process along with synthetic GCP generation is performed with the use of RAMP DEM which were uploaded with software.

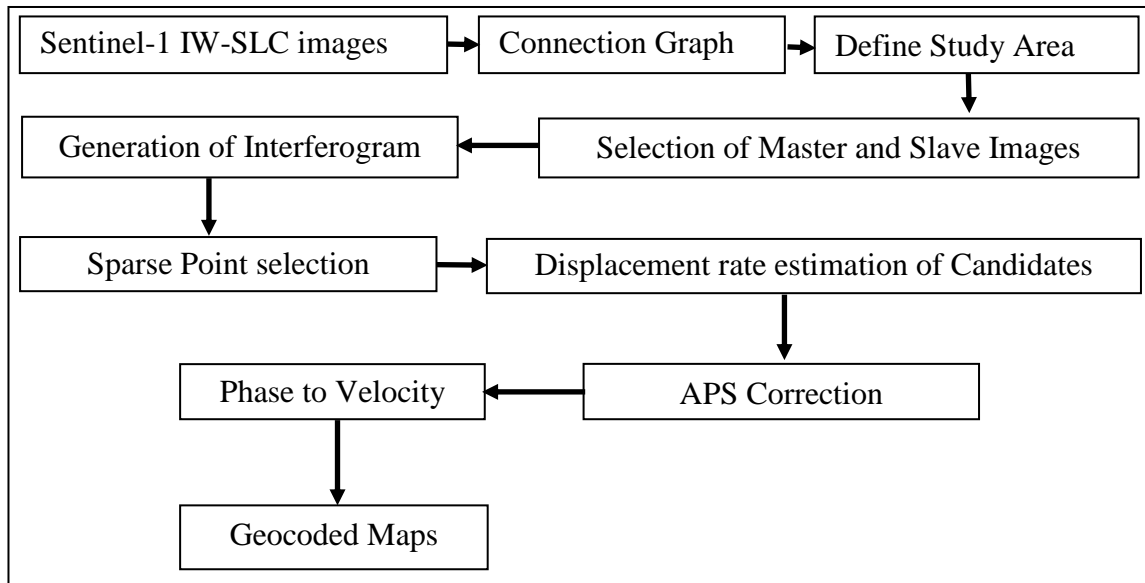


Figure 3. General steps for PS Interferometric process.

#### 4. RESULTS AND DISCUSSION

The velocity of Potsdam glacier is calculated with the help of six SAR images using PSInSAR. All the six images are alternatively used as master and slave, if one image is master rest of other behave as slave. In this study, we found similar behavior from image, if the coherence of master and slave is higher, then accuracy rate is higher. From this study, we found overall average velocity for this glacier as 45-60 m/yr, whereas at higher altitude toward the south west of the glacier flow is at 30-35 m/yr and at lower altitude it measured as 55-65 m/yr. Because of less coherence in some of the part of the glacier, we got biased result but it was low, so we removed it by defining a threshold value.

Table 2. Velocity output estimated using different images

Date of Image	Average Coherence (varies from 0 to 1)	Estimated average velocity (m/yr)
29-07-2016	0.95	32
10-08-2016	0.92	32
22-08-2016 (Master)	1	0
03-09-2016	0.98	37
15-09-2016	0.88	38
27-09-2016	0.96	34

#### 5. CONCLUSION

We were able to estimate velocity of the glacier using C-band sensor satellite with accurate result. In the case of Potsdam glacier, its average velocity is around 0.12 m/day and annually it varies from 30 to 60 m, because of variation in the elevation of glacier. The result showed a flow rate of about 55-65 m/yr at lower altitude, whereas at higher altitude the flow speed was 30-35m, toward the south west of the glacier. Using the PSInSAR method on Interferometric SAR data for estimating glacier velocity, the accuracy of the results varied according to the coherence level of the SAR images; those having higher coherence (> 0.92) were able to provide accurate results. As the coherence decreased, it was not easy to conduct study with the SAR images.

#### ACKNOWLEDGEMENT

The authors would like to thank Dr. Daniele Perissin, Assistant Professor at Purdue University for providing the software assistance. We are very thankful to the European Space Agency for making availability freely Sentinel-1 data. We also acknowledge Dr. Rajan, former Director, ESSO-NCAOR and Dr. M. Ravichandran, Director, ESSO-NCAOR, for their encouragement and motivation for this research.

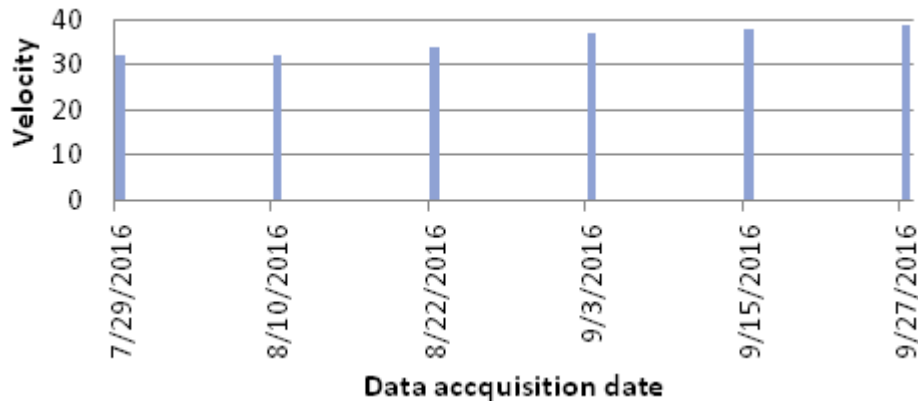


Figure 4. Estimated average velocity (m/yr).

## REFERENCES

- Alley, R., Blankenship, D., Bentley, C. and Rooney, S., 1986. Deformation of till beneath ice stream B, West Antarctica. *Nature*, 322(6074), pp.57-59.
- Anon, 2014. Proceedings of USAR 2014; 10th European Conference on Synthetic Aperture Radar. 1st ed. IEEE / Institute of Electrical and Electronics Engineers Incorporated.
- Anon, 2017. InSAR Principles: Guidelines for SAR Interferometry Processing and Interpretation, (ESA TM-19). [online] European Space Agency. Available at: ([http://www.esa.int/About\\_Us/ESA\\_Publications/InSAR\\_Principles\\_Guidelines\\_for\\_SAR\\_Interferometry\\_Processing\\_and\\_Interpretation\\_br\\_ESA\\_TM-19](http://www.esa.int/About_Us/ESA_Publications/InSAR_Principles_Guidelines_for_SAR_Interferometry_Processing_and_Interpretation_br_ESA_TM-19)) [Accessed 4 May 2017].
- Anschütz, H., Eisen, O., Oerter, H., Steinhage, D. and Scheinert, M., 2007. Investigating small-scale variations of the recent accumulation rate in coastal Dronning Maud Land, East Antarctica. *Annals of Glaciology*, 46(1), pp.14-21.
- Berardino, P., Fornaro, G., Lanari, R. and Sansosti, E., 2002. A new algorithm for surface deformation monitoring based on small baseline differential SAR interferograms. *IEEE Transactions on Geoscience and Remote Sensing*, 40(11), pp.2375-2383.
- Berthier, E., Vadon, H., Baratoux, D., Arnaud, Y., Vincent, C., Feigl, K., Rémy, F. and Legrésy, B., 2005. Surface motion of mountain glaciers derived from satellite optical imagery. *Remote Sensing of Environment*, 95(1), pp.14-28.
- Bürgmann, R., Rosen, P. and Fielding, E., 2000. Synthetic Aperture Radar Interferometry to Measure Earth's Surface Topography and Its Deformation. *Annual Review of Earth and Planetary Sciences*, 28(1), pp.169-209.
- Colesanti, C., Ferretti, A., Novali, F., Prati, C. and Rocca, F., 2003. Sar monitoring of progressive and seasonal ground deformation using the permanent scatterers technique. *IEEE Transactions on Geoscience and Remote Sensing*, 41(7), pp.1685-1701.
- De Zan, F. and Monti Guarnieri, A., 2006. TOPSAR: Terrain Observation by Progressive Scans. *IEEE Transactions on Geoscience and Remote Sensing*, 44(9), pp.2352-2360.
- Dietrich, R., Metzger, R., Korth, W. and Perlt, J., 1999. Combined use of field observations and SAR interferometry to study ice dynamics and mass balance in Dronning Maud Land, Antarctica. *Polar Research*, 18(2), pp.291-298.
- Ferretti, A., Prati, C. and Rocca, F., 2000. Nonlinear subsidence rate estimation using permanent scatterers in differential SAR interferometry. *IEEE Transactions on Geoscience and Remote Sensing*, 38(5), pp.2202-2212.
- Ghiglia, D. and Romero, L., 1994. Robust two-dimensional weighted and unweighted phase unwrapping that uses fast transforms and iterative methods. *Journal of the Optical Society of America A*, 11(1), p.107.

Goldstein, R. and Werner, C., 1998. Radar interferogram filtering for geophysical applications. *Geophysical Research Letters*, 25(21), pp.4035-4038.

Goldstein, R., Zebker, H. and Werner, C., 1988. Satellite radar interferometry: Two-dimensional phase unwrapping. *Radio Science*, 23(4), pp.713-720.

Harper, J., Humphrey, N., Pfeffer, W., Huzurbazar, S., Bahr, D. and Welch, B., 2001. Spatial variability in the flow of a valley glacier: Deformation of a large array of boreholes. *Journal of Geophysical Research: Solid Earth*, 106(B5), pp.8547-8562.

Hartl, P. and Bamler, R., 1998. Synthetic aperture radar interferometry. *Inverse Problems*, 14(4), pp.R1-R54.

Hellwich, O. and Ebner, H., 2000. Geocoding SAR interferograms by least squares adjustment. *ISPRS Journal of Photogrammetry and Remote Sensing*, 55(4), pp.277-288.

Ivanov, S., Ishihara, T., Brown, B., Müller, R. and Gaina, C., 2007. Breakup and early seafloor spreading between India and Antarctica. *Geophysical Journal International*, 170(1), pp.151-169.

Jawak, S., Bidawe, T. and Luis, A., 2015a. A Review on Applications of Imaging Synthetic Aperture Radar with a Special Focus on Cryospheric Studies. *Advances in Remote Sensing*, 04(02), pp.163-175.

Jawak, S.D., Luis, A.J., 2014. Prospective application of NASA-ISRO SAR (NISAR) in cryospheric studies: a practical approach, NISAR Science Workshop, 17-18 November, Space Applications Centre (SAC), Ahmedabad, Gujarat, India. DOI: 10.13140/RG.2.1.1587.5687. [Oral]

Jawak, S.D., Luis, A.J., 2015c. Potential of SAR imagery for mapping and monitoring iceberg calving events in Antarctic environment, XII International Symposium on Antarctic Earth Science (ISAES 2015), Abstract No. S22-13, pp. 487. DOI: 10.13140/RG.2.1.3062.1285.

Jawak, S.D., Luis, A.J., 2015d. NASA-ISRO SAR (NISAR) imagery for monitoring iceberg calving events in the Antarctic environment, NISAR Science Workshop, 19-20 November, Space Applications Centre (SAC), Ahmadabad, Gujarat, India. [Poster]

Jawak, S.D., Panditrao, S.N., and Luis, A.J., 2015b. RISAT-1 C-band dual polarimetric SAR imagery for classification of cryospheric features in Antarctic environment, XII International Symposium on Antarctic Earth Science (ISAES 2015), Abstract No. S22-8, pp. 482, Goa, India, July 13-17, 2015. DOI: 10.13140/RG.2.1.5159.2807.

Joughin, I., Kwok, R. and Fahnestock, M., 1996. Estimation of ice-sheet motion using satellite radar interferometry: method and error analysis with application to Humboldt Glacier, Greenland. *Journal of Glaciology*, 42(142), pp.564-575.

Kenyi, L. and Kaufmann, V., 2003. Estimation of rock glacier surface deformation using sar interferometry data. *IEEE Transactions on Geoscience and Remote Sensing*, 41(6), pp.1512-1515.

Massonnet, D. and Feigl, K., 1998. Radar interferometry and its application to changes in the Earth's surface. *Reviews of Geophysics*, 36(4), pp.441-500.

Mattar, K., Vachon, P., Geudtner, D., Gray, A., Cumming, I. and Brugman, M., 1998. Validation of alpine glacier velocity measurements using ERS Tandem-Mission SAR data. *IEEE Transactions on Geoscience and Remote Sensing*, 36(3), pp.974-984.

Prats-Iraola, P., Rodriguez-Cassola, M., De Zan, F., Scheiber, R., Lopez-Dekker, P., Barat, I. and Geudtner, D., 2015. Role of the Orbital Tube in Interferometric Spaceborne SAR Missions. *IEEE Geoscience and Remote Sensing Letters*, 12(7), pp.1486-1490.

Rignot, E. and Kanagaratnam, P., 2006. Changes in the Velocity Structure of the Greenland Ice Sheet. *Science*, 311(5763), pp.986-990.

Rignot, E., Bamber, J., van den Broeke, M., Davis, C., Li, Y., van de Berg, W. and van Meijgaard, E., 2008. Recent Antarctic ice mass loss from radar interferometry and regional climate modelling. *Nature Geoscience*, 1(2), pp.106-110.

Rosen, P., Hensley, S., Joughin, I., Li, F., Madsen, S., Rodriguez, E. and Goldstein, R., 2000. Synthetic aperture radar interferometry. *Proceedings of the IEEE*, 88(3), pp.333-382.

Scheuchl, B., Flett, D., Caves, R. and Cumming, I., 2004. Potential of RADARSAT-2 data for operational sea ice monitoring. *Canadian Journal of Remote Sensing*, 30(3), pp.448-461.

Strozzi, T., Luckman, A., Murray, T., Wegmuller, U. and Werner, C., 2002. Glacier motion estimation using SAR offset-tracking procedures. *IEEE Transactions on Geoscience and Remote Sensing*, 40(11), pp.2384-2391.